

copies (siISG15). Supernatants collected at different times post-infection were used to infect fresh cells. After 24 hours, the RNAs were extracted from the cells and expression of HCV RNA was determined by RTqPCR. (E) Huh7.25.CD81 cells, transfected with 25 nM of siRNA (Control or ISG15) for 48 hrs, were infected with JFH1 for the times indicated. Cell extracts were analysed by immunoblot with Abs directed against ISG15, MAVS, the HCV NS3 and core proteins and Actin as loading control.
doi:10.1371/journal.ppat.1002289.g002

domain (DRBD) of PKR [8], while unaffected by C16, a chemical compound which inhibits the catalytic activity of PKR (Figure 5D). In line with this, PRI but not C16, abrogated the ability of HCV to induce ISG15 (Figure 5E). The same result was obtained for induction of ISG56 (Figure S10). We then used human primary hepatocytes (HHP) to determine whether HCV

was also able to induce ISGs through PKR in a more physiological cellular model. A follow-up of the infection over a period of 96 hours showed that JFH1 was replicating correctly in those cells as well as leading to induction of ISG15 (10-fold) and to some induction of IFN β (2.5-fold). These cells were infected with JFH1 for 8 hours in the absence or presence of PRI, making convenient

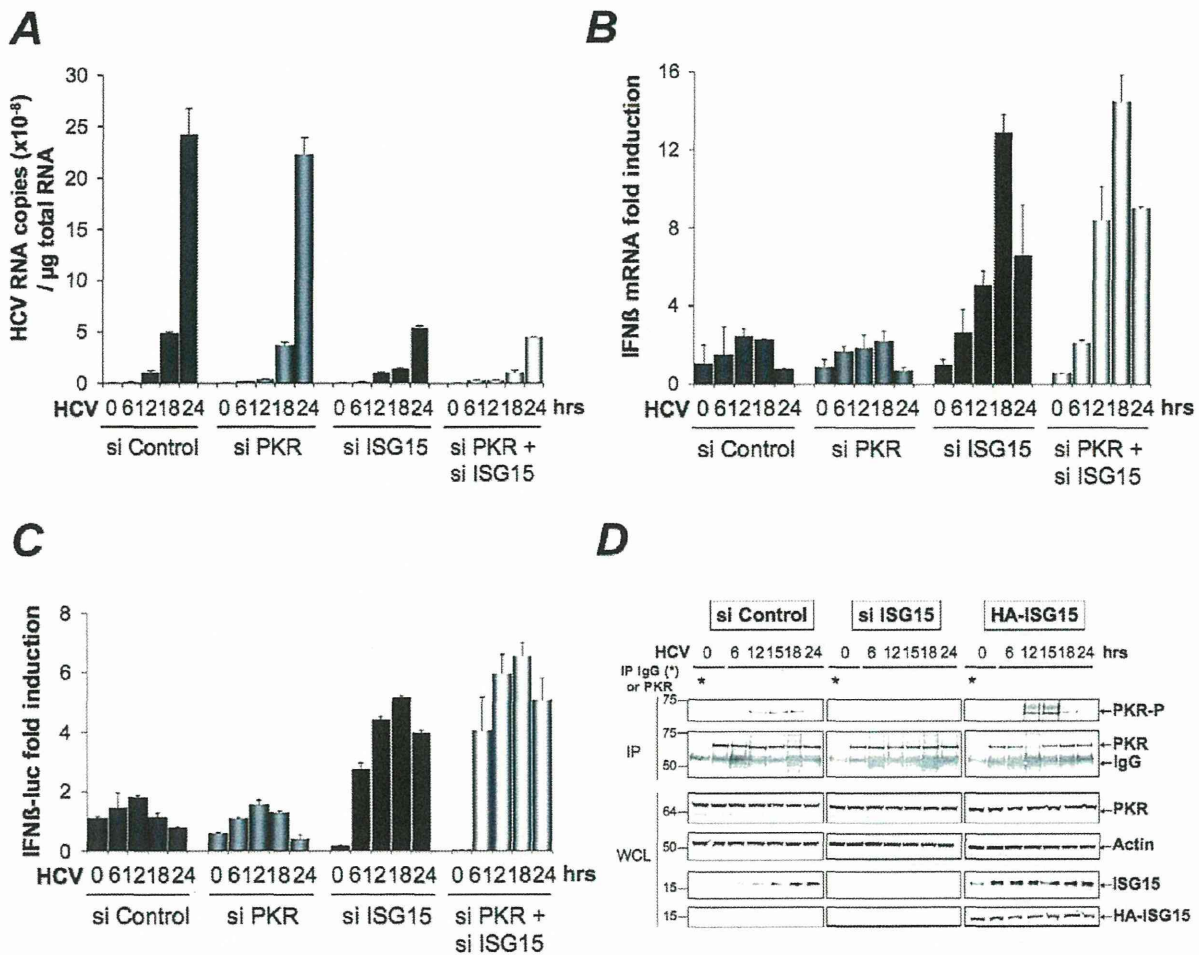


Figure 3. ISG15 strengthens the pro-HCV activity of PKR. (A–B). The Huh7.25.CD81 cells were transfected with 25 nM of the different siRNA (Control, ISG15, PKR), separately or together. After 48 hrs, cells were infected with JFH1 (m.o.i = 0.2). At the times indicated, expression of HCV or IFN β RNA was determined by RTqPCR and expressed as copies of JFH1 RNA (A) or as fold induction (IFN β ; B). The expression levels of IFN β RNA at the start of infection was 6.96×10^5 copies. (C) Two sets of Huh7.25.CD81 cells were first transfected with siRNA ISG15, siRNA PKR separately and together for 24 hrs, then transfected with the reporter plasmids IFN β -firefly luciferase (pGL2-IFN β), pRL-TK Renilla-luciferase for another 24 hrs and infected with JFH1 (m.o.i = 0.2) for the times indicated. In each case, IFN expression was expressed as fold-induction over control cells that were simply transfected with pGL2-IFN β -FLUC/pRL-TK-RLUC. The graph represents the level of firefly luciferase activity normalized to the ratio R-luc RNA/GAPDH RNA. Such normalization is required because of the negative control of general translation through PKR after 12 hrs post-infection [8]. Error bars represent the mean \pm S.D for triplicates. (D) Huh7.25.CD81 cells, in 100 cm² plates, were transfected with siRNA Control or siRNA ISG15 or transfected with a plasmid expressing HA-ISG15 for 48 hrs and infected with JFH1 (m.o.i = 6). At the indicated times post-infection, cell extracts (2.2 mg) were processed for immunoprecipitation of PKR or for incubation with mouse IgG as a control of specificity (asterisk). The immunoprecipitated complexes were run on two different NuPAGE gels and blotted using Mab 71/10 or anti-phosphorylated PKR antibodies (PKR-P). The presence of PKR and PKR-P was revealed using the Odyssey procedure. The ratio PKR-P/PKR in the absence or in the presence of ISG15, either endogenous or endogenous and ectopic, is shown in Figure S5.
doi:10.1371/journal.ppat.1002289.g003

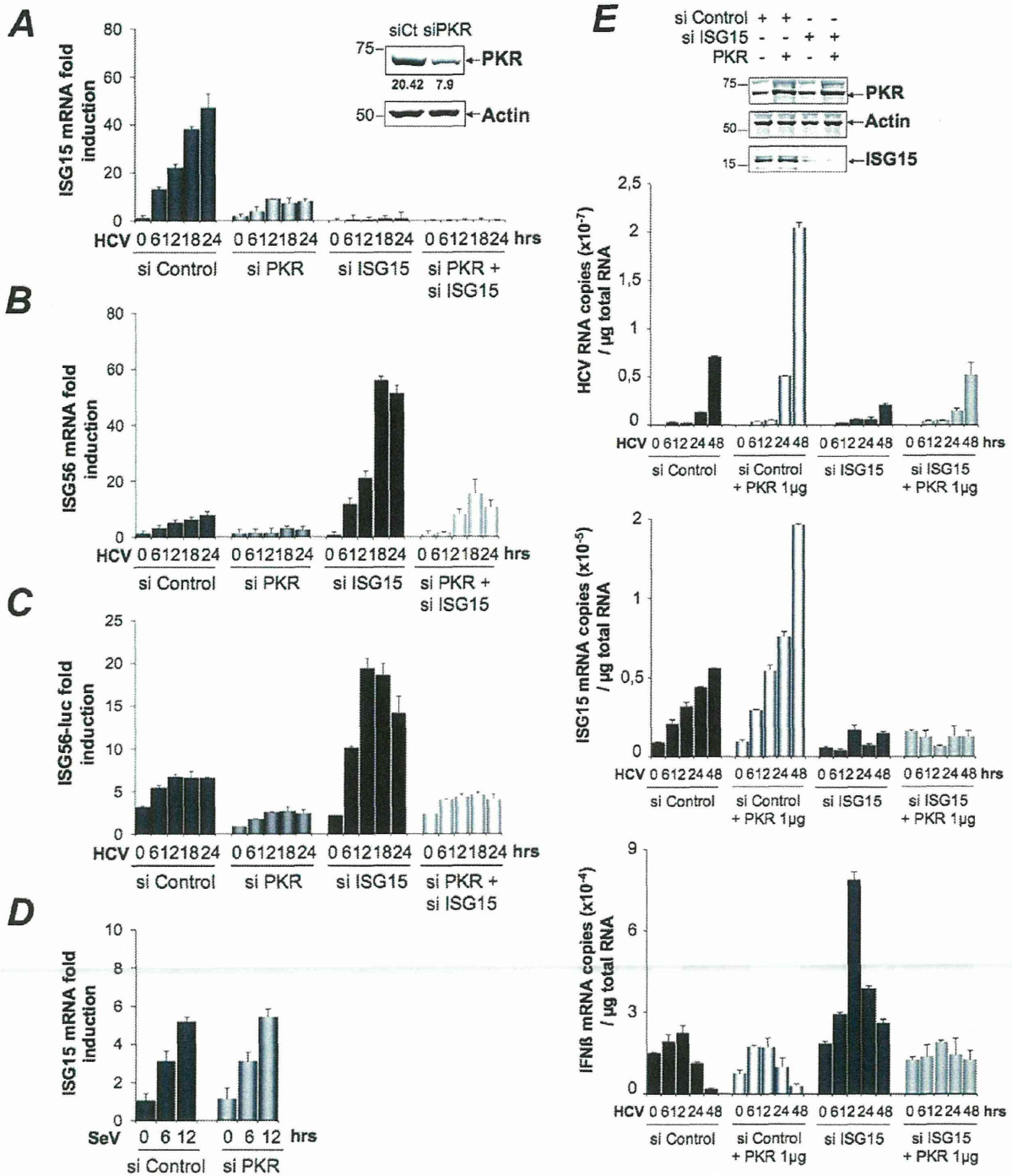


Figure 4. HCV triggers a PKR-dependent pathway early in infection to induce ISG15 and other genes. (A–C) The cDNAs reverse transcribed from the RNAs extracted from the Huh7.25.CD81 cells for the experiment described under Figure 3A were analysed by qPCR for the expression of ISG15 (A) and ISG56 (B). Expression levels of ISG15 and ISG56 RNA at the start of infection were respectively 1×10^5 and 1.18×10^5 copies. A novel set of Huh7.25.CD81 cells were transfected with siRNA Control, siRNA ISG15, siRNA PKR separately and together for 48 hrs. They were then transfected with the reporter plasmids ISG56-FLUC and pRL-TK-RLUC and infected with JFH1 (m.o.i.=0.2). At the times indicated, the effect of the different conditions of silencing on the reporter expression was analyzed after normalization performed as described under Figure 3C (C). Results are expressed as fold induction. Error bars represent the mean \pm S.D for triplicates. (D) Huh7.25.CD81 cells were either transfected with 25 nM of siRNA Control or siPKR for 24 hrs and infected with SeV for the times indicated. Expression of endogenous ISG15 was determined by RTqPCR and expressed as fold induction. Error bars represent the mean \pm S.D for triplicates. The expression levels of ISG15 RNA at the start of infection were respectively 4.91×10^4 copies (siControl) and 5.44×10^4 copies (siPKR). (E) Huh7.25.CD81 cells were either transfected with 25 nM of siRNA Control or

siISG15 and with 1 μ g of a plasmid expressing PKR where indicated. After 48 hrs, the cells were infected with HCV (m.o.i.=6) for the times indicated. Expression of HCV, ISG15 and IFN β RNA was determined by RTqPCR. Cell lysates prepared from cells treated in the same conditions but not infected were used to control expression of PKR and ISG15 by immunoblot.
doi:10.1371/journal.ppat.1002289.g004

use of the cell-penetrating ability of this peptide. Longer period of treatment with PRI were not investigated for practical reasons (see Materials and Methods). The results showed that PRI was significantly inhibiting the induction of ISG15 while it had no effect on that of IFN β (Figure 5F). Altogether, these data demonstrate that HCV triggers induction of early ISGs through MAVS and TRAF3 by using PKR as an adapter protein.

PKR interacts both with MAVS and TRAF3 and binds HCV RNA ahead of RIG-I

The ability of HCV to control activation of the RIG-I/MAVS pathway after induction of ISG15 through a novel PKR/MAVS pathway suggests that PKR has the possibility to bind MAVS prior to RIG-I. To determine this, we established the kinetics of these interactions, after treating the Huh7.25.CD81 cells with siRNAs targeting ISG15 prior to HCV infection. This was necessary in view of the negative control of ISG15 on RIG-I. MAVS was immunoprecipitated from the cell extracts at different times post-infection and the presence of PKR and RIG-I was examined in the immunocomplexes, as well as that of TRAF3, used as marker of activation of the MAVS signaling pathway. As expected, only PKR was able to associate with MAVS and TRAF3 in the control cells (Figure 6A) whereas both PKR, RIG-I and TRAF3 were found in the immunocomplexes in the absence of ISG15 (Figure 6B). The PKR/MAVS association took place at 4 hrs post-infection in the control cells but was observed 2 hrs earlier in the ISG15-depleted cells. Whether ISG15 plays a role in the regulation of the PKR/MAVS association remains to be determined. However, the presence of TRAF3 in association with MAVS at 2 hrs post-infection in the control cells (Figure 6A) correlates with its association with PKR (Figure 5C) which indicates that the MAVS pathway can be activated through PKR as soon as 2 hrs post infection. In ISG15 knock-down cells, the RIG-I/MAVS association occurred later at 6 hrs post-infection with an increase in TRAF3 association at 9–12 hrs post infection. Altogether, these data revealed that HCV infection triggers an earlier interaction of MAVS with PKR than with RIG-I.

Finally, we asked whether PKR was able to associate with HCV RNA and how this association can be compared to that of RIG-I. PKR and RIG-I were immunoprecipitated at 2, 4 and 6 hrs post-infection and the presence of HCV RNA was analysed in the complexes. The results showed that PKR associates with HCV RNA with best efficiency at 2 hrs post-infection. Importantly, this association was strongly inhibited in presence of PRI, thus confirming the importance of PKR DRBD in the process. In contrast, the association of HCV RNA with RIG-I was detected only at 6 hrs post-infection. Interestingly, the association between RIG-I and HCV RNA was not affected by PRI, which rules out the possibility that the initial formation of a complex between PKR and HCV RNA was a pre-requisite for the subsequent binding of RIG-I to HCV RNA. Immunoprecipitation of PKR at 1, 2, 4 and 6 hrs post-infection, in presence of an inhibitor of ribonucleases also did not lead to detection of RIG-I in the complexes (Figure S11). Association of HCV RNA with eIF2 α , used as negative control, was not significant, thus showing the specificity of the assay (Figure 6C). Whether a direct interaction of PKR with HCV RNA represents the initial event leading to the MAVS-dependent induction of early ISGs remains now to be characterized. Altogether, these data reveal an earlier mobilization

of PKR than RIG-I in response to HCV infection which leads to activation of a MAVS-dependent signaling pathway.

Discussion

Hepatitis C virus can attenuate IFN induction at multiple levels in infected hepatocytes, such as through the NS3/4A-mediated MAVS cleavage [7,27] and by using the eIF2 α kinase PKR to control IFN and ISG expression at the translational level [8,9]. Here, we have identified another process by which HCV controls IFN induction at the level of RIG-I ubiquitination through ISG15 and an ISGylation process. Importantly, we have shown that ISG15 is rapidly induced, among other ISGs, in response to HCV infection, through a novel signaling pathway that involves PKR, MAVS, TRAF3 and IRF3 but not RIG-I. In this pathway, PKR is not used for its kinase function but rather as an adapter protein with its dsRNA binding domain (DRBD) playing an essential role in this mechanism (Figure 7). By transcriptome analysis, we showed that HCV induces a number of ISGs in the HCV-permissive Huh7.25.CD81 cells and we confirmed the induction of two of these, ISG15 and ISG56, in other HCV-permissive cells, such as Huh7.5 and Huh7 cells. In addition, induction of ISG15 by HCV in a PKR-dependent manner was confirmed in human primary hepatocytes. The ability of HCV to trigger high expression levels of ISG15 and ISG56, as well as other ISGs, has previously been reported in models of HCV-infected chimpanzees [10,12,28] and in HCV-infected patients [14,15,16]. Induction of ISGs thus represents a general propriety of the response of the cells to HCV. In addition to this, natural variations in intra-hepatic levels of ISG15 *in vivo* may increase the susceptibility of some patients to HCV infection. The ability of HCV to control RIG-I activity through ISG15 is important to note in view of several reports which highlight the importance of a role for ISG15 in the maintenance of HCV in livers [15,16] or in the control of HCV replication in cell cultures [17,25]. Our data provide an explanation for the presence of ISGs at high expression levels in HCV-infected patients [14,15,16] and in models of HCV-infected chimpanzees [10,12,28] in the absence of, or with poor IFN expression.

The 15 Kda ISG15, or Interferon Stimulated Gene 15 [29], also known as ubiquitin cross reactive protein (UCRP) [30], can be conjugated (ISGylation) to more than 150 cellular protein targets [31] through the coordinated action of three E1, E2 and E3-conjugating enzymes, in a process similar but not identical to ubiquitination. While both ubiquitin and ISG15 can use the same E2 enzyme UbcH8, Ube1L functions as a specific E1 enzyme for ISG15, in spite of its 45% identity with Ube1, the E1 enzyme for ubiquitin [32]. The major E3 ligase for human ISG15 is HERC5 [33].

Interestingly, RIG-I was identified as a target for ISG15, among other IFN-induced proteins or proteins involved in IFN action [31]. However, its activity appears to be negatively controlled by ISG15 and the ISGylation process, either as shown previously after cotransfection with the ISG15 and the ISG15-conjugating enzymes [18] or as shown here, in a model of infection with HCV. Indeed, ISG15 is now emerging as playing a proviral role in case of HCV infection. Several reports now highlight the importance of a role for ISG15 in the control of HCV replication in cell cultures [17,25] as well as in the maintenance of HCV in livers and

Table 1. PKR-dependent up-regulated genes upon HCV infection.

siPKR mock/siCt	Name	Access. N.	siCtMock	siCt HCV	siCtMock'	siPKRHCV	LOG2*
0,6	ISG56	NM_001548	15,0	885,8	10,2	7,6	-6,3
0,7	ISG15	NM_005101	593,6	26061,9	410,6	283,5	-6,0
0,7	IFI 9-27/IFITM1	NM_003641	27,8	817,7	15,1	10,1	-5,5
1,2	IFI1-8U	NM_006435	24,0	597,7	10,9	7,2	-5,3
1,1	Olfactory Receptor 9l1	NM_001005211	26,6	473,1	10,1	4,8	-5,2
1,6	IFI1-8U	XM_084845	17,7	365,4	9,3	6,5	-4,9
0,8	OASp100	NM_006187	46,4	909,9	40,0	33,5	-4,5
0,8	IFI6-16	NM_002038	834,5	10040,6	45,9	24,1	-4,5
0,6	Ub2L6	NM_004223	392,7	4078,9	281,2	128,7	-4,5
0,9	OAS 1	NM_016816	49,9	704,03	31,8	21,6	-4,4
0,9	ISG12	NM_005532	46,3	592,54	38,3	29,2	-4,1
0,8	IFP 35	NM_005533	36,3	369,7	26,6	16,9	-4,0
0,6	PARP-9	NM_031458	29,5	318,5	37,8	25,6	-4,0
0,5	GABA-B receptor 1	NM_006398	29,5	500,8	26,0	28,5	-4,0
0,7	Lysp100B	NM_003113	8,7	93	8,5	6,1	-3,9
0,8	PDIP1	NM_033405	27,4	146,6	28,0	12,8	-3,6
0,8	PKR	NM_002759	48,2	306,8	47,0	26,0	-3,5
1,6	MT-IM	NM_176870	49,0	1371,8	6,9	19,6	-3,3
0,7	Phospholipid scramblase	NM_021105	170	1137,2	189,9	153	-3,1
1,1	RIG-I	NM_014314	23,5	223,2	18,9	21,9	-3,0
0,6	IFIT-5	NM_012420	24,9	95,3	35,0	21,3	-2,7
1,3	RIG-I	NM_004585	7,4	42,5	6,3	6,0	-2,6
0,7	STAT1 beta	NM_139266	336,9	1401,5	300,3	210,3	-2,6
0,8	BRCA1 C-ter assoc. Prot	NM_001040444	12,3	45,1	8,1	5,1	-2,6
0,9	Cohesin Rec8 homolog	NM_005132	18,0	103	16,7	16,9	-2,5
0,5	C/EBPdelta	NM_005195	324,9	901,8	278,9	161,27	-2,3
0,7	ZNF532	NM_018181	32,8	146,5	25,5	23,8	-2,3
0,6	NNMT	NM_006169	52,8	143,8	50,26	28,9	-2,2
1	ISG1-8U	XM_084845	32,0	146,8	23,1	22,7	-2,2
1,1	HIF00	NM_153833	45,3	199,9	34,7	32,9	-2,2
0,8	ISG20	NM_002201	129,3	338,3	107,5	61,4	-2,2
1,1	PSMB10	NM_002801	16,2	75,1	14,5	15,0	-2,2
1,3	ZC3HAV1	NM_024625	8,3	26,0	6,9	4,9	-2,1
0,9	SOD2	NM_000636	348,5	1612,2	311	334,3	-2,1
0,7	PARP12	NM_022750	269,9	875,2	296,9	224,2	-2,1
0,7	NMI	NM_004688	32,1	136	37,4	37,0	-2,1
0,8	NEDD9	NM_006403	5,7	19,0	5,7	4,7	-2,0
1,1	SAMHD1	NM_015474	17,1	49,5	13,6	9,7	-2,0
0,7	AKT2	NM_001626	13,4	20,0	14,2	5,4	-2,0
0,5	ARG1	NM_000045	245,9	282,6	231,4	67,0	-2,0
0,8	BHLHB2	NM_003670	76,4	128,0	71,5	30,5	-2,0
0,8	LGALS3BP	NM_005567	22,0	72,0	16,1	13,6	-2,0
1,3	ZNF292	XM_048070	22,3	31,4	20,2	7,3	-2,0
1,1	STAT1	NM_007315	53,3	275,3	48,2	64,9	-1,9
0,7	TBA3_HUMAN	NM_006009	28,2	43,6	33,4	13,7	-1,9
0,5	TM4SF20	NM_024795	45,2	51,0	36,9	11,1	-1,9
1,4	ERAP2	NM_022350	9,8	19,2	8,8	4,6	-1,9
0,8	USP18	XM_001126794.1	215,1	979,2	201,8	245,9	-1,9
1	USP18	XM_001126794.1	129,6	617,0	127,3	165,5	-1,9

Table 1. Cont.

The Huh7.25.CD81 cells, seeded at 3×10^6 cells in 10-cm plates, were transfected after 24 hrs with 25 nM of siRNA Control or siRNA PKR using Eugene HD. 24 hrs post transfection, they were either mock-infected or infected for 2 hrs at 37°C with JFH1 (moi=0.2) (three independent plates/sample). The medium was then removed and cells were incubated with complete DMEM for 12 hrs at 37°C. The cells were washed twice with TBS containing phosphatase and protease inhibitors, harvested by scraping, the cell pellets were centrifuged, the supernatants were removed and the pellets were frozen and stored at -80°C before being processed for micro-array. The list shows genes that were affected no more than twice by the depletion of PKR in the control cells ($0.5 < \text{siPKR mock/siCt} < 1.6$). The dependence of each of these genes in regards with PKR for their induction by HCV is expressed as \log_2 (ratio (siPKR HCV/siCt Mock) - (siCt HCV/siCt Mock)) (indicated by \log_2^*) with a cut-off of ≈ 2.0 fold.

doi:10.1371/journal.ppat.1002289.t001

pinpoint ISG15 as among the predictor genes of non-response to IFN therapy [14,15,16].

At present, we do not know at which level ISGylation regulates IFN induction in response to HCV infection. An HCV-mediated increase of ISG15 would favour preferential binding of ISG15 over that of ubiquitin to the E2 enzyme UbcH8 and hence enhance the spatio-temporal availability of UbcH8-ISG15 for HERC5 over that of UbcH8-ubiquitin for TRIM25. It may also lead to inhibition of TRIM25, through autoISGylation [21,34], which would decrease its ability to ubiquitinate RIG-I. We showed that overexpression of HERC5 together with Ube1L, UbcH8 and ISG15 was increasing the ability of ISG15 to inhibit IFN induction by HCV (**Figure 2B**). All three enzymes Ube1L, UbcH8 and HERC5 belong to the family of genes induced by IFN and it has been reported that ISGylation is optimum in a context of IFN treatment [18,35]. Therefore, it is tempting to speculate that elevated levels of ISG15 in some HCV-infected patients would bring the most favourable context for the virus when those patients are under IFN therapy. This would be in accord with the clinical data showing that HCV-induced high expression of ISG act as a negative predictive marker for response to IFN therapy.

It is doubtful that viruses with high IFN-inducing efficiency, such as Sendai virus may control RIG-I through ISG15 and PKR. However, viruses that avoid inducing IFN may have use of the PKR pathway. A good example might be that of Hepatitis B Virus (HBV) [36,37,38]. PKR expression was previously reported to be elevated in HCC liver from chronically HBV infected patients [39] and a relationship between PKR and IFN induction during HBV infection would be important to evaluate.

At present, we have established that HCV RNA interacts with PKR as soon as 2 hours post-infection. This interaction occurs prior the interaction of HCV RNA with RIG-I, which suggests that PKR may rapidly detect structures containing the incoming HCV RNA genome. Indeed, PKR has been reported to bind the dsRNA domains III and IV of HCV IRES [40] in addition to its ability to also bind 5' triphosphorylated ss or dsRNA structures [41]. Whether PKR behaves as a pathogen recognition receptor for HCV RNA, like RIG-I, remains to be clarified. It is however clear that, in contrast to RIG-I, PKR acts here in favour of the pathogen rather than in favour of the host defense. We have established that the HCV RNA/PKR interaction depends on the first DRBD present at the N terminus of PKR and is independent on its kinase activity. The ability of PKR to serve as adapter in signaling pathways is not a total surprise since it has been previously shown to activate NF- κ B through interaction of its C terminus with members of the TRAF family, such as TRAF5 and TRAF6 [42]. PKR contains also TRAF interacting motif in its N terminus [42] and an association between TRAF3 and PKR has been reported upon cotransfection in 293T cells [43]. Intriguingly, PKR was previously reported to participate in the induction of IFN β , in association with MAVS, through activation of NF- κ B or ATF-2 but not or partially IRF3; however these studies were not

performed in the absence of RIG-I [44,45,46]. The mode of interaction between PKR, TRAF3 and MAVS, independently of RIG-I, and how it leads to a preferential induction of ISGs and not of IFN β in response to HCV infection in contrast with the RIG-I/MAVS pathway remains to be determined. Based on our data, we propose now to divide the innate response to acute HCV infection into two phases: an early acute phase in which PKR is activated and a late acute phase that depends on RIG-I, the early phase controlling activation of the late phase. It is now essential to progress towards the generation of specific pharmaceutical inhibitors targeting PKR in order to abrogate the early acute phase to the benefit of the RIG-I-driven late phase. In a more general view, care should now be taken in the choice of compounds designed to be used as immune adjuvants, such as to be devoid of activation of the early acute PKR phase. This will ensure their efficiency as to activate properly the innate immune response through the late acute RIG-I phase.

Methods

Cell cultures and viruses

The culture of Huh7, Huh7.5, Huh7.25.CD81 cells, the preparation of Sendai virus stocks (≈ 2000 HAU/ml) and of HCV JFH1 stocks ($\approx 6.10^4$ FFU/mL and $\approx 6.10^6$ FFU/mL) was as described [8,47]. Preparation and cultures of human primary hepatocytes was as described [48]. Of note, the ability of the Huh7.25.CD81 cells to induce IFN in response to SeV without prior IFN treatment (40-fold) was not observed in our previous study [8]. The ability of Sendai virus to induce IFN is related to the presence of copyback DI (Defective Interfering) genomes [49]. The higher IFN inducing ability of the novel Sendai virus stock may have come from an important accumulation of these copyback DI genomes, during its growth in chicken eggs.

PKR inhibitors

The C16 compound [50] and the cell-permeable PRI peptide [51] were provided by Jacques Hugon. These drugs were applied (200 nM for C16 and 30 mM for PRI) one hour before the end of the 2 hr- incubation time with JFH1 and re-added to the medium after washing the cells with phosphate buffered saline (PBS). Note that PRI loses its effect very rapidly, probably through degradation in the cells, and requires to be added every hour to the cells until the end of treatment.

Expression vectors

TRIM25 was cloned from the IFN-treated Huh7.25CD81 cells (500 U/ml IFN- α 2a; Cellsciences) after RT-PCR using the forward: 5'-ATGGCAGAGCTGTGCCCCCT-3' and reverse 5'-CTACTTGGGGGAGCAGATGG-3' primers. The pcDNA3.1(+) vector expressing 5'HA tagged-TRIM25 (provided by D. Garcin; University of Geneva, Switzerland) was used to generate the TRIM25 P₃₅₈L construct by site-directed mutagenesis. The

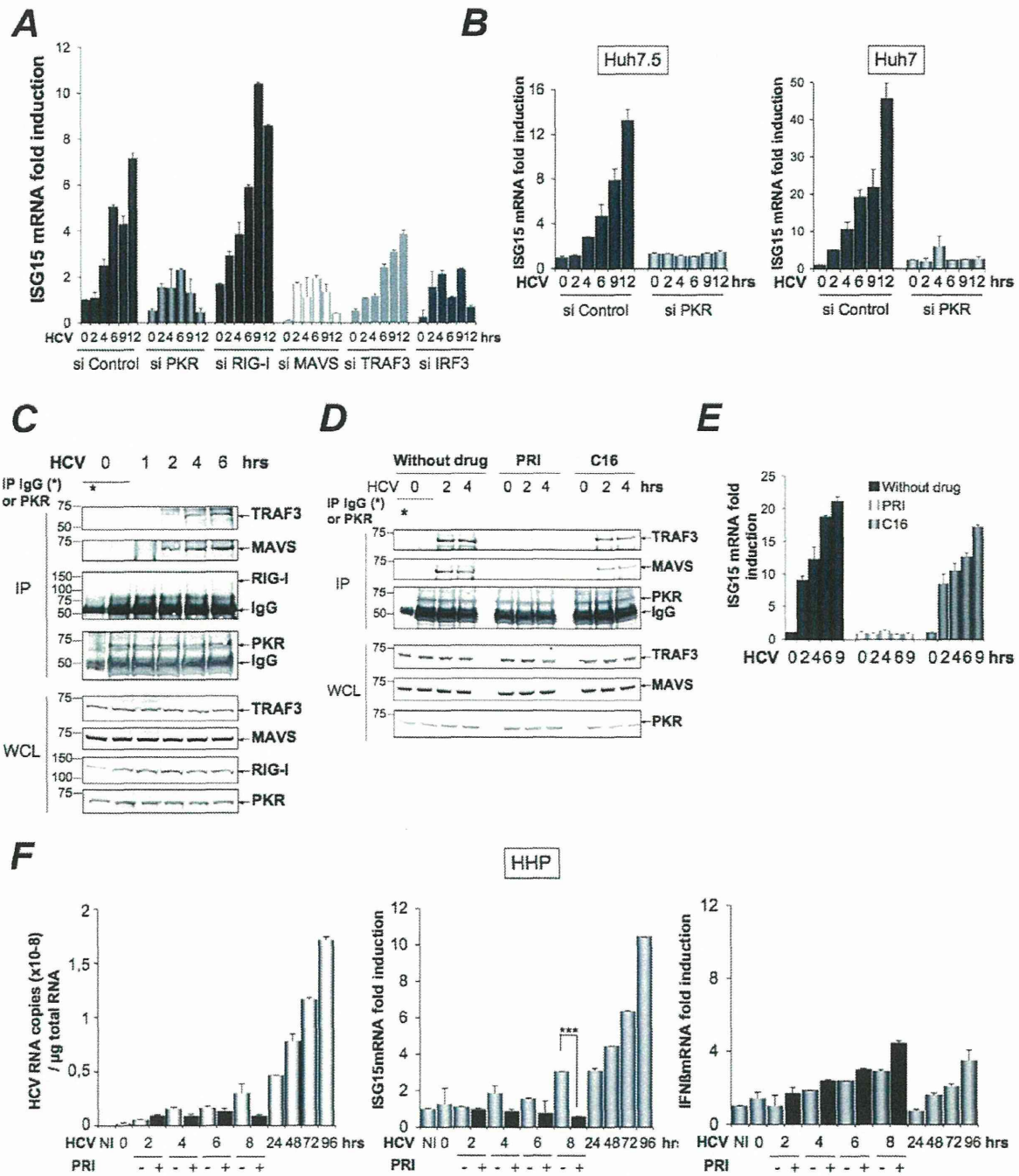


Figure 5. HCV-dependent induction of ISG15 involves PKR, MAVS and TRAF3 and not RIG-I. (A–B). A–The Huh7.25.CD81 cells were transfected with 50 nM Control siRNA and the different Smartpool siRNAs (50 nM siPKR; 10 nM siRIG-I; 5 nM siMAVS; 50 nM siTRAF3; 50 nM siIRF3) for 48 hrs and infected with JFH1 (m.o.i.=6). (B) Huh7.5 or Huh7 cells were transfected with siRNA Control or siPKR (50 nM) for 48 hrs and infected with JFH1 (m.o.i.=0.2 for Huh7.5 or 10 for Huh7). At the times indicated, expression of endogenous ISG15 was determined by RTqPCR and expressed as fold induction. Error bars represent the mean \pm S.D for triplicates. The expression level of ISG15 RNA at the start of infection in the siControl cells was 9.97×10^4 copies (Huh7.25.CD81), 1.31×10^4 copies (Huh7.5) and 1.28×10^4 (Huh7). (C–D) Huh7.25.CD81 cells, in 100 cm² plates, were infected with JFH1 (m.o.i.=0.2) alone (C) or in presence of PRI or C16 (D). At the times indicated, cell extracts (3.5 mg) were processed for immunoprecipitation of PKR or for incubation with mouse IgG as a control of specificity (asterisk). The detection of the proteins in the complexes and in the whole cell extracts (WCE) was revealed by immunoblot using the Odyssey procedure. (E) The Huh7.25.CD81 cells were incubated with PRI or C16 and infected with JFH1 (m.o.i.=0.2) for the times indicated. Expression of endogenous ISG15 was determined as in A–B. The ISG15 RNA levels were 3.81×10^4 copies in the siControl cells. (F) Human primary hepatocytes (HHP) were infected with JFH1 (m.o.i.=6). One set of cells was incubated with 30 mM of the PRI inhibitor during 8 hours. At the times indicated, expression of HCV RNA, ISG15 and IFN β was determined by RTqPCR. The expression levels of ISG15 and IFN β RNA at the start of infection was 1.05×10^5 copies and 1.11×10^4 copies, respectively. Inhibition of induction of ISG15 by PRI at 8 hr post-infection was statistically significant (***, p=0.0001). doi:10.1371/journal.ppat.1002289.g005

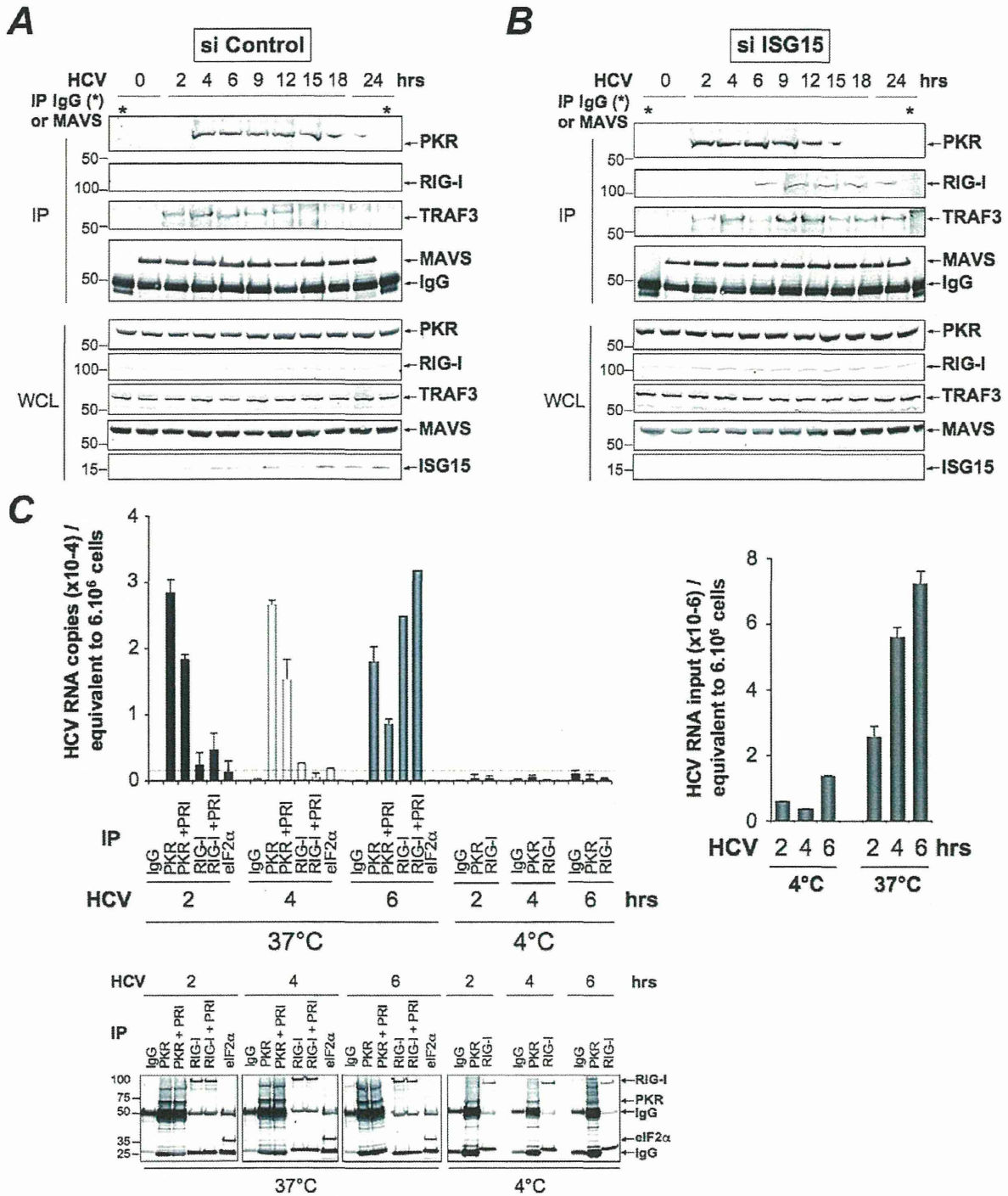


Figure 6. PKR both interacts with MAVS and TRAF3 and binds HCV RNA ahead of RIG-I. (A–B)– Huh7.25.CD81 cells were transfected with 25 nM of siRNA Control (A) or 25 nM of siRNA ISG15 (B) for 48 hrs and infected with JFH1 (m.o.i=0.2). At the times indicated, cell extracts (4.5 mg) were incubated with anti-MAVS antibodies. In addition, cell extracts prepared at 0 hr post-infection were incubated with mouse IgG as a control of specificity (asterisk). The immunoprecipitated complexes were run on three different NuPAGE gels and blotted using Mab 71/10, anti-MAVS, anti-RIG-I or anti-TRAF3 antibodies. The expression level of each protein was controlled in the total cell extracts. (C)– Huh7.25.CD81 cells were incubated with JFH1 (m.o.i=6) for 2 hrs at 37°C or at 4°C in the absence or presence of 30 μ M of PRI. This drug was applied one hour before the end of the incubation time. After washing the cells twice with PBS, the cells were further incubated for 2, 4 or 6 hrs at 37°C or at 4°C in the absence or presence of PRI (added every hour). The cell extracts were processed for crosslinking of RNA to proteins before lysis, as described in Materials and Methods and different immunoprecipitations were performed with antibodies directed against PKR, RIG-I or eIF2 α . After extensive washing, the presence of HCV RNA linked to the immunocomplexes was analysed by RTqPCR and the presence of the proteins was verified by Western blot. Measure of HCV RNA in

the cell extracts allowed to estimate its percentage of binding to PKR as 1.09%, 0.47% and 0.25% at 2, 4 and 6 hrs post-infection respectively, and its percentage of binding to RIG-I as 0.34% at 6 hrs post-infection.
doi:10.1371/journal.ppat.1002289.g006

IFN β -firefly luciferase (pGL2-IFN β) and pRL-TK Renilla-luciferase reporter plasmids were described previously [8]. The pGL3 luciferase reporter construct containing the -3 to -654 nucleotides of the ISG56 promoter was provided by N.Grandvaux [52]. The Myc-HIS-Ubiquitin construct was provided by R.Kopito (Stanford University, CA). ISG15 was cloned from IFN-treated Huh7 cells using the forward: 5'-GGATCCCATGGGCTGGGACCTGACGGTG-3' and reverse 5'-CTCGAGCTCCGCCCGCCAGGCTCTGT-3' primers and inserted into the pcDNA3.1(+)/HA vector. The Ube1L, UbcH8 and HERC5 constructs were kindly provided by Jon M. Huijbregtse [35]. The

pcDNA1/AMP vector expressing PKR has been described previously [53].

RNA-mediated interference

The siRNAs directed against PKR, MAVS, RIG-I, TRAF3 and IRF3 which were used for the experiment described in figure 5A correspond to pools of siRNA (Smartpool) obtained from Dharmacon Research, Inc. (Lafayette, CO), as well as siRNAs directed against Ube1L used in Figure 2B. Control (scrambled) siRNA and siRNA directed against PKR or ISG15, used in all other experiments, were chemically synthesized by Dharmacon

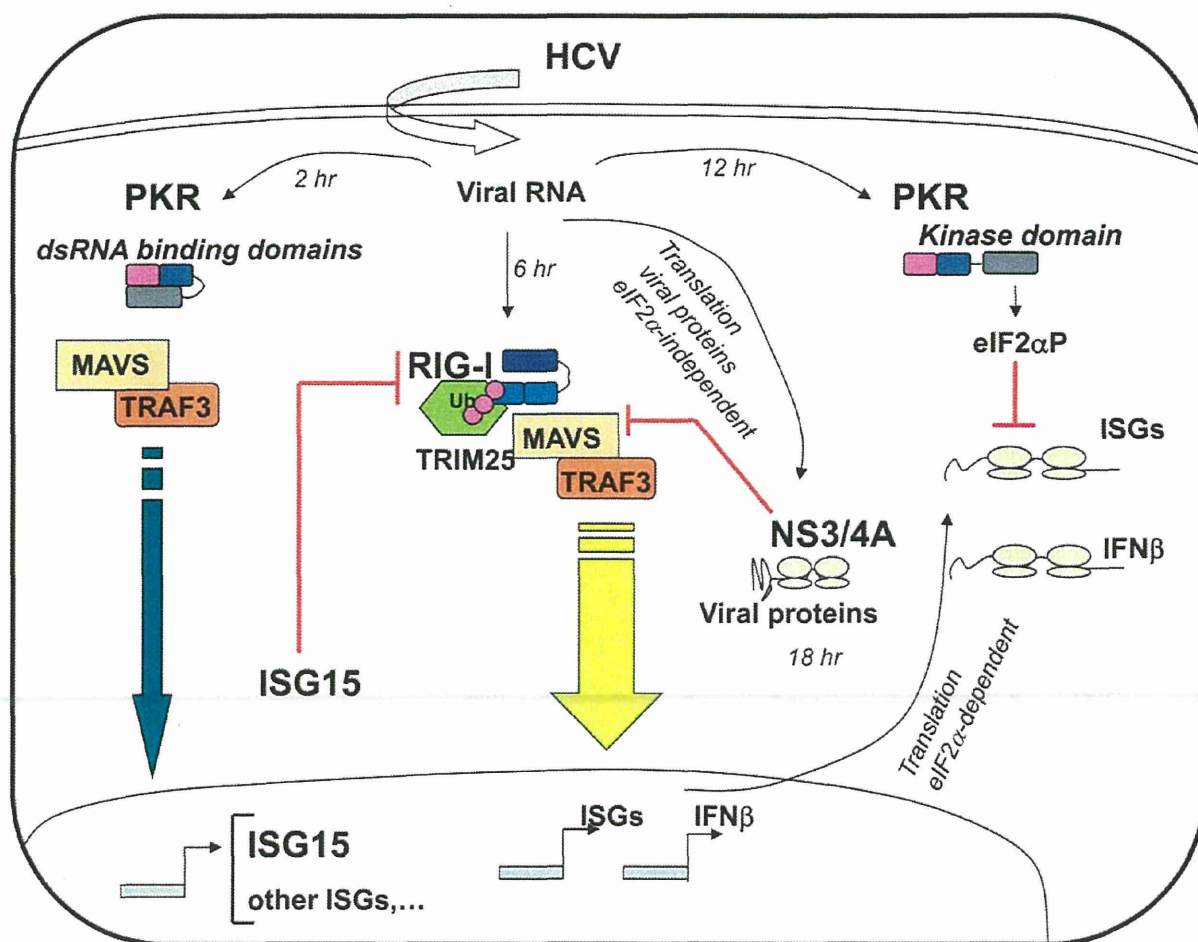


Figure 7. Multiple levels of control of IFN induction during HCV infection. Soon after infection, the HCV RNA is detected by the dsRNA binding domains (DRBD) of PKR ahead (2 hr) of its recognition by the RNA helicase RIG-I (6 hr). Recruitment of PKR by HCV triggers a signaling pathway that involves PKR as an adapter protein to recruit MAVS and TRAF3. This leads to a strong induction of the di-ubiquitine like protein ISG15 as well as other IRF3-dependent ISGs (Interferon-Stimulated Genes). ISG15 negatively controls the TRIM25-mediated ubiquitination (Ub) of RIG-I through an ISGylation process and thus interferes with the ability of RIG-I to recruit its downstream partners, including MAVS and TRAF3, and to induce IFN β and ISGs. As the infection proceeds, HCV activates the eIF2 α kinase function of PKR (12 hr). This leads to a transient (few hours) inhibition of general translation, including that of IFN [8] and ISGs [9] while the eIF2 α -independent translation of the viral proteins proceeds unabated. At later times in the infection (18 hr), additional control of IFN induction occurs through cleavage of MAVS by the HCV NS3/4A protease, once the viral proteins have sufficiently accumulated in the cytosol [7,27].
doi:10.1371/journal.ppat.1002289.g007

(scrambled and PKR) and by EUROFINS MWG Operon (ISG15) (Text S1). The siRNAs (final concentration 25 nM or 50 nM) were transfected for 48 h using jetPRIME reagent according to the manufacturer's instructions (PolyPlus transfection TM) before transfection with other plasmids or before infection.

Antibodies

Mab to ISG15 (clone 2.1) was a kind gift of E. Borden [54]. Mab to PKR was produced from the murine 71/10 hybridoma (Agrobio; Fr) with kind permission of A.G. Hovanesian [55]. Other antibodies were as follows: anti-mouse IgG (Santa Cruz), anti-TRAF3 (Santa Cruz), pThr451-PKR (Alexis), MAVS (Alexis), anti-actin (Sigma), anti-pSer10-Histone H3 (Millipore), anti-HCV NS3 (Chemicon), anti-HCV core (Thermo scientific), anti-RIG-I (Alexis Biochemical Inc.), anti-TRIM25 (6105710; BD Bioscience), anti-IRF3 (Santa Cruz), anti-HA (12CA5; Roche) and anti-Myc (Santa Cruz).

Reporter assays

Huh7.25.CD81 cells (80,000 cells/well; 24-well plates) were transfected with 40 ng of pRL-TK Renilla-luciferase reporter (Promega) and 150 ng of either pGL2-IFN β -Firefly luciferase reporter or pISG56-luciferase reporter and processed for dual-luciferase reporter assay as reported previously [8].

Real-time RT-PCR analysis

Total cellular RNA was extracted using the TRIZOL reagent (Invitrogen). HCV RNA was quantified by one-step RTqPCR. Reverse-transcription, amplification and real-time detection of PCR products were performed with 5 μ l total RNA samples, using the SuperScript III Platinum one-step RTqPCR kit (Invitrogen) and an AbiPrism 7700 machine. For the sequence of the different primers, see Text S1. The results were normalized to the amount of cellular endogenous GAPDH RNA using the GAPDH control kit from EuroGentec. Copies number of HCV RNA may vary due to internal calibration and depending on the preparation of the viral stocks. All m.o.i were calculated using the titers expressed in FFU/ml. The IFN β , ISG15, ISG56, Ube1L and GAPDH amplicons were quantified by a two-step RTqPCR assay as described [8].

Transcriptome analysis

Cellular RNA was extracted and purified from the cells using RNAeasy mini kit (QIAGEN K.K., Tokyo, Japan). Comprehensive DNA microarray analysis was performed with 3D-Gene Human Oligo chip25k with 2-color fluorescence method by New Frontiers Research Laboratories, Toray Industries Inc, Kamakura, Japan as previously described [56]. In brief, each sample was hybridized with 3D-Gene chip. Hybridization signals were scanned using Scan Array Express (PerkinElmer, Waltham, MA). The scanned image was analyzed using GenePix Pro (MDS Analytical Technologies, Sunnyvale, CA). All the analyzed data were scaled by global normalization.

Immunoprecipitation and immunoblot analysis

Cells were washed once with PBS and scraped into lysis buffer 1 (50 mM TRIS-HCl [pH 7.5], 140 mM NaCl, 5% glycerol, 1% CHAPS) that contained phosphatase and protease inhibitors (Complete, Roche Applied Science). The protein concentration was determined by the Bradford method. For immunoprecipitation, lysates were incubated at 4°C overnight with the primary antibodies as indicated and then in the presence of A/G-agarose beads (Santa Cruz Biotechnology) for 60 minutes. The beads were

washed three times, and the precipitated proteins were extracted at 70°C using NuPAGE LDS sample buffer. Protein electrophoresis was performed on NuPAGE 4–12% Bis TRIS gels (Invitrogen). Proteins were transferred onto nitrocellulose membranes (Biorad), and probed with specific antibodies. Fluorescent immunoblot images were acquired and quantified by using an Odyssey scanner and the Odyssey 3.1 software (Li-Cor Biosciences) as described previously [8]. For detection of ISG15, cells were lysed in RIPA buffer (50 mM TRIS-HCl [pH 8.0]; 200 mM NaCl; 1% NP-40; 0.5% Sodium Deoxycholate; 0.05% SDS; 2 mM EDTA) and protein electrophoresis was performed on 4–20% polyacrylamide gels (PIERCE).

Nuclear/cytoplasmic extract

Pellets from cells washed in ice-cold phosphate-buffered saline (PBS) were lysed in ice-cold cytoplasmic buffer (10 mM TRIS [pH 8.0], 5 mM EDTA, 0.5 mM EGTA, 0.25% Triton X-100) containing phosphatase and protease inhibitors. The suspension was centrifuged for 30 seconds at 14,000 g and the supernatant (cytoplasmic fraction) was transferred into microcentrifuge tubes. The nuclear pellet was resuspended in Urea buffer (8 M Urea, 10 mM TRIS [pH 7.4], 1 mM EDTA, 1 mM dithiothreitol) containing phosphatase and protease inhibitors, homogenized by vortex and boiled for 10 minutes. The protein concentration was determined by the Bradford method.

Ubiquitination assay

Huh7.25.CD81 cells were transfected for 48 hrs with 5 μ g of Myc-His-Ubiquitin expression plasmid using jetPRIME reagent. The cells were then washed in ice-cold PBS containing 20 mM N-ethylmaleimide (Sigma-Aldrich), harvested directly in Gua8 buffer (6 M guanidine-HCl, 300 mM NaCl, 50 mM Na₂HPO₄, 50 mM NaH₂PO₄ [pH 8.0]), briefly sonicated, and centrifuged at 14,000 g for 15 min at 4°C. 1/10th of the lysate was subjected to precipitation with 10% trichloroacetic acid for protein analysis in whole cell extracts. The rest of the lysate was incubated for 2 hrs with 20 μ l (packed volume) of Talon resin Ni-affinity beads (Clontech) on a rotating wheel. Bound proteins were washed four times in Gua8 buffer, three times in Urea 6.3 buffer (8 M Urea, 10 mM TRIS, 0.1 M Na₂HPO₄, 20 mM Imidazole [pH 6.3]), and three times in cold PBS, after which they were eluted by boiling in NuPAGE LDS sample buffer. Electrophoresis was performed on 4–12% of acrylamide NuPAGE gels (Invitrogen).

Co-precipitation protein/HCV RNA

Huh7.25.CD81 cells were incubated for 10 min in their culture medium containing 1/10 volume (Vol) of a crosslinking solution (11% Formaldehyde, 0.1 M NaCl, 1 mM Na-EDTA-[pH 8], 0.5 mM Na-EGTA-[pH 8], 50 mM HEPES [pH 8]). The reaction was stopped by addition of a solution of 0.125 M glycine in PBS [pH 8] at room temperature (RT). The cells were washed three times in ice-cold PBS containing 1000 U/ml of RNase inhibitor (Promega), scraped in PBS and dispatched into three sets containing 1/2 (set 1), 1/4 (set 2) and 1/4 (set 3) of the cell suspension. The three sets were centrifuged for 30 seconds at 14,000 g and 4°C and the cell pellets were lysed into lysis buffer 1 containing phosphatase/protease and RNase inhibitors (Promega) for sets 1 and 2 or into TRIZOL reagent for set 3. Cell lysates from sets 1 and 2 were then incubated at 4°C, first overnight with the appropriate primary antibodies and for 60 minutes in the presence of A/G-agarose beads (Santa Cruz Biotechnology). After the incubation period, the beads were washed four times with buffer 1. Set 1 (HCV RNA bound to immunocomplexes) and set 3 (input HCV RNA) were submitted to TRIZOL treatment and HCV